The Topology of the Universe

Contents

1 Introduction

Ideas regarding the shape of the universe are probably as old as humanity. At least since ancient Greek times, people have wondered whether space is finite or infinite in extent. Since only Euclidean geometry, describing an unbounded space, was known at the time, it was tacitly assumed that finiteness implied the existence of a boundary. Although these matters were of some philosophical interest, the constraints of technological and mathematical possibility would render them inaccessible to physical inquiry for centuries to come. Luckily, around 1830 non-Euclidean geometry was discovered and with the formulation of Riemannian geometry in 1854, the theoretical framework was finally present to describe spaces and their shapes.

The course of history seems to prove a striking human preoccupation with flat Euclidean space over curved non-euclidean spaces. During the 20th century, the discovery of General Relativity inspired great skepticism toward the Euclidean model, though in the end it seems to have managed to withstand all attempts at its falsification. Recent empirical methods, especially the WMAP, have ruled out more and more possible curvature, but Euclidean space remains safely inside of our confidence intervals. The evidence in favor of flat space is at best as compelling as the evidence against it, however, and the only thing we can be certain of is that our space is very close to being flat (compared to what?).

In 2003, an analysis of periodicity in the cosmic microwave background (CMB) led Jean-Pierre Luminet to suggest that the universe is a topological space known as the Poincaré dodecahedral space (PDS). As will be shown, this implies a spherical geometry, in stark contrast to the concordance model of cosmology.

In this thesis, I will explore the credibility of the Poincaré dodecahedral space as a model for our universe and I will also attempt to illuminate the methods by which such a model can be verified, or more realistically falsified. To accomplish these goals, section 2 will be a quick introduction to 3-dimensional topology and its geometries. For the sake of brevity, this thesis will then focus on the Poincaré dodecahedral space, disregarding all other geometries and manifolds. Section 3 is dedicated to proving that the Poincaré dodecahedral space does in fact result from identifying faces of a dodecahedron in a certain way. To do this, I will systematically rule out all other possibilities for the shape of the tessellation of S^3 representing the PDS. In section 4, I will try to explain the merits of the PDS model in explaining physical data, meaning mostly the WMAP data on the CMB. During this section, four known ways of detecting cosmic topology will be addressed; searching for duplicates, circles in the sky, cosmic crystallography, and the CMB quadrupole. This This section will be the climax to my argument and will hopefully put the previous sections to good use. The main results and lack thereof will, as per convention, be stated in section 5, which will conclude the paper.

2 Geometries on 3-Manifolds

This section will treat the different homogeneous geometries possible on 3-manifolds and the manifolds that allow them. To enable a treatment of these subjects, a number of definitions must first be stated.

First of all, the meaning of the term geometry should be established. Choosing a suitable definition for geometry is vital here, as different approaches exist. Due to the differential geometric nature of general relativity, the mathematical results will ultimately have to be stated in terms of Riemannian geometry. To do this, a metric has to be introduced, which is mathematically much to stringent to describe manifold geometries. For example, scaling the metric should not affect the perceived geometry, whereas in a Riemannian sense it does. A more natural notion in this case is given by Kleinian geometry, which presupposes isometries, rather than metrics. Luckily, Kleinian geometry, though weaker in its assumptions, is often equivalent to Riemannian geometry up to scaling. For the sake of readability, the term geometry will therefore be taken to imply Kleinian geometry.

Definition 1. A geometry is a tuple (S, G), consisting of a space S and a group G working transitively on S. Furthermore, $\forall x \in S$, the point stabiliser $G_x = \{g \in G | gx = x\}$ of x under G must be compact.

In definition 1, G is implied to be the group of isometries of S. Notice that if, for $x \in S$, $\phi_x : G \to S : g \mapsto gx$ is defined to be a group homomorphism (by defining the suitable group operation on S) and the stabilizer $G_x = \{g \in G : gx = x\}$, we get $G/G_x = \phi_x/\ker \phi_x \cong \operatorname{im} \phi_x = S$ by transitivity of G on S. Also, as this definition requires G to be transitive on S, geometries in the Kleinian sense are always homogeneous. From a mathematical point of view, this is somewhat restrictive compared to general Riemannian geometry, but from a physical point of view, this is a very natural constraint. Note also that, although the definition requires all stabilizers to be compact, it is in fact sufficient for the stabilizer of one individual point to be compact, since all geometries are homogeneous.

For the definition of a manifold, I will closely follow Thurston [10]. A manifold will be a structure locally resembling $\mathbb{R}^n$, for some fixed n. The exact form of this local resemblance determines the intrinsic structure of the manifold.

Definition 2. An n-dimensional manifold is a tuple $(\mathcal{M}, A)$, where $\mathcal{M}$ is a topological space and the atlas A is a collection of coordinate charts (U_i, ϕ_i). Furthermore $\cup_i U_i = \mathcal{M}$ and $\phi_i : U_i \to \mathbb{R}^n$ are all homeomorphisms.

Note that according to this definition, different atlases on the same space $\mathcal{M}$ always define different manifolds. It should be clear, however, that a manifold can be given many atlases, while retaining essentially the same structure. Also, this definition allows manifolds of very general structure, most of which will not be able to carry a geometry at all.

The first problem is mainly a technical detail, and will not be very relevant in this paper. To address it, we have to specify what exactly is meant by essential structure, which brings us to the second problem.

In this article, geometries on manifolds will be considered, so the essential structure mentioned before should clearly be geometrical. To establish this, the definition of a general manifold needs to be narrowed down a little to the notion of a geometric manifold.

Definition 3. An n-dimensional geometric manifold is a 3-tuple $(\mathcal{M}, A, G)$, such that $(\mathcal{M}, A)$ is a manifold and $g_{i,j} : \phi_i^{-1}(U_i \cap U_j) \to \phi_j(U_i \cap U_j) : \phi_i(x) \mapsto \phi_j(x) = g|_{U_i \cap U_j}$ for some $g \in G$, for all i, j.

Where again G is implied to be the group of isometries, but of the geometry as modelled in $\mathbb{R}^n$. Finally, there is need for a definition stating what it means for a manifold to admit a certain geometric structure.

Definition 4. A model geometry is a geometry (S, G), where S is a simply connected space and G is no proper subgroup of any group H for which (S, H) is a geometry.

Definition 5 will now state what is meant by admitting a geometry.

Definition 5. A manifold F is said to admit a geometry modelled on some model geometry (S, G) if $\exists \Gamma < G : S/\Gamma \cong F$ and $S \to S/\Gamma$ is a covering map.

The condition that $S \to S/\Gamma$ is a covering map leads to the more practical condition that Γ must be properly discontinuous and act freely on S, which for compact S reduces to Γ being finite. Now the stage is set for a look at the different kinds of geometries that occur in 3-dimensional manifolds.[9]

To examine the possible model geometries, we need to examine the possible groups G that can occur. Here we have great advantage of the local euclidean nature of manifolds. Since G is defined to consist locally of isometries on the parameter space $\mathbb{R}^3$, we already know that the point stabilisers of G are point stabilisers of $\mathbb{R}^3$. Specifically we see that the stabiliser G_x has to be a subgroup of O(3), so it needs to be the product of O(1), O(2) or O(3) by some finite group.

In the case of $O(3)$ itself, we have an isotropic geometry.

2.1 Isotropic Geometries

The first case to consider is the case where G_x is O(3). In this case the resulting geometry is by definition isotropic. Since any two planes in the tangent space are equivalent under SO(3) symmetry, the metric must be a constant. The metric can then be scaled to $-1, 0, 1$ according to it's sign, leading to the three well-known homogeneous isotropic spaces.

2.1.1 $\mathbb{E}^3$

First of these homogeneous isotropic geometries is Euclidean 3-space $\mathbb{E}^3$. The group of isometries of $\mathbb{E}^3$ is aptly called the Euclidean group, which will be denoted by $I(\mathbb{E}^3)$. $I(\mathbb{E}^3)$ can be equated to $\mathbb{R}^3 \rtimes O(3)$ were $\mathbb{R}^3$ and $O(3)$ are taken to act canonically on $\mathbb{E}^3$ and the action of $O(3)$ on $\mathbb{R}^3$ is also taken to be canonical.

As it turns out, there are exactly ten manifolds admitting $\mathbb{E}^3$ geometry. To find these manifolds, one must find freely acting discrete subgroups of $I(\mathbb{E}^3)$. This can easily, but laboriously be done by simply trying all 230 crystallographic groups, as seems to have been done by Werner Nowacki.[10]

These ten manifolds can be conveniently described as fibre bundles over 2 dimensional orbifolds[9], but this would take us to far astray.

2.1.2 $\mathbb{H}^3$

Second of the homogeneous isotropic geometries is $\mathbb{H}^3$. To find the isometries of $\mathbb{H}^3$, consider the upper half space representation of $\mathbb{H}^3$. The isometries of $\mathbb{H}^3$ are generated by reflections in geodesics, which are represented as circles orthogonal to the horizontal plane (vertical lines being considered as an extreme case). By definition, a reflection in a circle is an inversion and the transformations generated by these inversions are the Möbius transformations. In other words, $I(\mathbb{H}^3) = \mathrm{PSL}(2, \mathbb{C})$, the Möbiusgroup.

The manifolds admitting a $\mathbb{H}^3$ geometry are as diverse as they are numerous and their classification is an ongoing process.

2.1.3 $\mathbb{S}^3$

Last of the homogeneous isotropic geometries is $\mathbb{S}^3$. As opposed to $\mathbb{H}^3$, $\mathbb{S}^3$ can be embedded in $\mathbb{R}^4$, which saves some effort in describing its geometrical properties. $\mathbb{S}^3$ is described by the unit sphere in $\mathbb{R}^4$, so $I(\mathbb{S}^3)$, its group of isometries is $O(4)$.

Like the hyperbolic case, spherical geometry has infinitely many manifolds admitting its structure. Spherical geometries are a lot better behaved, though, as they can be divided into five families.

Lens spaces are the manifolds $\mathbb{S}^3/\Gamma$, were Γ is a cyclic subgroup of $SO(4)$. The element of Γ would then take the form

$$\begin{pmatrix} \cos(2\pi i/p) & -\sin(2\pi i/p) & 0 & 0 \\ \sin(2\pi i/p) & \cos(2\pi i/p) & 0 & 0 \\ 0 & 0 & \cos(2\pi i q/p) & -\sin(2\pi i q/p) \\ 0 & 0 & \sin(2\pi i q/p) & \cos(2\pi i q/p) \end{pmatrix}$$

for some relatively prime p, q, as operators on $\mathbb{S}^3$ embedded in $\mathbb{R}^4$. These spaces can be acquired by identifying the 'northern' and 'southern' hemihyperspheres along the boundary after turning them q/p relatively.

Prism manifolds are manifolds $\mathbb{S}^3/\Gamma$ for which Γ is one of certain metacyclic groups.

Polyhedral manifolds are manifolds $\mathbb{S}^3/\Gamma$ for which $\Gamma = P \times C_n$, for a binary polyhedral group P and certain cyclic groups C_n. A binary polyhedral group is the preimage of the corresponding polyhedral group under the two to one surjective homomorphism $\mathrm{SU}(2) \to \mathrm{SO}(3)$ Since there are three polyhedral groups T, O, and I, this leads to three more families of spherical 3-manifolds.

Lens spaces, Prism manifolds and three kinds of Polyhedral manifolds lead as claimed to exactly five families of spherical 3-manifolds. The most important spherical manifold for the purposes of modelling actual space is one of these prism manifolds. This manifold is called the Poincar'e Dodecahedral Space (PDS) or the Poincaré Homology Sphere and is given by $\mathbb{S}^3/I^*$, where I^* is a central extension of the icosahedral group I by two. Section 3 will be dedicated to proving that the fundamental domain for this space is in fact dodecahedral.

2.2 Fibred Two-Dimensional Geometries

As mentioned, another possibility for the stabiliser group of a geometrical manifold is $O(2)$. $O(2)$ as a subgroup of $O(3)$ is characterised by a one dimensional invariant subspace of T_xM, on which $O(3)$ acts. These invariant vectors in the tangent bundle of M define a unit vector field, which is G-invariant. The flow of this vector field defines integral curves which foliate M, as every point $x \in M$ has such an invariant vector and no two flows can cross. Since neighbourhoods of points on these curves are invariant under $O(2)$ perpendicular to the curve, there can not be two distinct points on the curve arbitrarily close perpendicularly. If this were the case, then the orbits of these points under $O(2)$ should be circles, and by continuity we would have a 2 dimensional tube-like structure, not a curve. This means that the leaves of this foliation are 1 dimensional submanifolds of M, i.e. $\mathbb{R}$ or S^1. If the foliation described here is factored out, what is left is a two-dimensional manifold B that inherits the Riemannian metric of M in a natural way. The integral curves described are now interpreted as fibres, leaving M a fibre bundle over B.

The connection on this bundle now determines the type of manifold described. This connection has a curvature form, which must be constant, since the group of isometries preserves it and acts transitively. By scaling and choosing orientation for the fibre, the curvature can, without loss of generality, be assumed to be either zero or one.

For a vanishing curvature, the bundle becomes trivial and there remain but three possibilities.

2.2.1 $\mathbb{S}^2 \times \mathbb{R}$

Firstly, the quotient space given by dividing the fibre out of the manifold could be S^2. The fibre is, as stated, given by $\mathbb{R}$ or S^1, leaving $\mathbb{S}^2 \times \mathbb{R}$ and $\mathbb{S}^2 \times S^1$ as

our manifolds. The second is covered by the first, leaving the geometry to be $\mathbb{S}^2 \times \mathbb{R}$.

This immediately leads us to a compact manifold admitting this geometry, namely $S^2 \times S^1$.

2.2.2 $\mathbb{H}^2 \times \mathbb{R}$

Secondly, the base space of our fibre bundle could be H^2. The fibre bundle would then of course be $\mathbb{H}^2 \times \mathbb{R}$ or $\mathbb{H}^2 \times S^1$, where again the case of the S^1 fibre is covered by the $\mathbb{R}$ bundle.

Examples of compact manifolds admitting $\mathbb{H}^2 \times \mathbb{R}$ include products of any compact hyperbolic surface with S^1.

For the third case mentioned the base space has to be $\mathbb{E}^2$. This base space, however, fibred by $\mathbb{E}$ in a trivial way leads to $\mathbb{R}^3$. $\mathbb{R}^3$ is of course a degenerate case, as it 'accidentally' has O(3) stabilisers instead of merely O(2). This is by definition equivalent to the isotropy of $\mathbb{R}^3$, which means that this geometry was already covered, and further digression is redundant.

This leaves us with three more cases to consider for which the connection on M has non-zero curvature. Let's start again by considering S^2 as a candidate base space for the fibre bundle. For reasons going beyond the scope of this paper, the resulting group of symmetries is not maximal with compact stabilisers. This means that no model geometry can be constructed this way

2.2.3 $\mathrm{SL}_2\mathbb{R}$

Taking the base space to be H^2 will prove a more fruitful endeavour. Now, the unit tangent bundle is $PSL(2, \mathbb{R})$, the orientation preserving subgroup of the isometry group of $\mathbb{H}^2$. The universal cover of this group will be called $\mathrm{SL}_2\mathbb{R}$ and is thus the desired geometry.

As is shown by the construction above, the universal cover of the unit tangent bundle of any compact hyperbolic surface is a manifold admitting $\mathrm{SL}_2\mathbb{R}$ geometry.

2.2.4   Nil

Finally, also E^2 must be considered as a base space. The way to construct a non trivial fibre of $\mathbb{R}$ over $\mathbb{R}^2$ is to consider the geometry of the Heisenberg group. The Heisenberg group is given by

$$
\begin{pmatrix}
1 & x & y \\
0 & 1 & z \\
0 & 0 & 1
\end{pmatrix}
$$

for $x, y, z \in \mathbb{R}$.

Manifolds admitting this geometry can be classified neatly as Seifert fibre spaces.

2.3 Solve geometry

Left to consider is the possibility of trivial point stabilisers. Now, it is clear that since G acts transitively and has trivial stabilisers it can be identified with the manifold M. This means that the remaining cases, or case actually, can be found examining all Lie groups not covered by the previous seven geometries.

Consider some basis (e_1, e_2, e_3) of the Lie algebra of the Lie group under consideration. The Lie bracket is a linear map on the Lie algebra that turns out to be Hermitian with respect to the cross product. A well known result from linear algebra then tells us that this operator representing the Lie bracket has three orthonormal eigenvectors. Taking these orthonormal vectors as a basis (e_1, e_2, e_3) it will be clear that:

$$[e_i, e_j] = L(e_i \times e_j) = L(\pm e_k) = \pm \lambda_k e_k$$

where $i \neq j \neq k \neq i$, L is the operator identified with the Lie bracket and λ_k is the eigenvalue of L corresponding to the eigenvector e_k. By scaling the basis to $(a_1 e_1, a_2 e_2, a_3 e_3)$, the previous result becomes:

$$[e_i, e_j] = L(e_i \times e_j) = L(\pm \frac{a_i a_j}{a_k} e_k) = \pm \lambda_k \frac{a_i a_j}{a_k} e_k$$

So that the structure constants can effectively be rescaled to zero or plus or minus one. Also, the elements of the basis may be freely permuted, permuting also the structure constants. Odd permutations will change some signs though, due to the anti-symmetry of the operations involved.

This leaves us with a small number of cases to consider.

$\lambda_1 = \lambda_2 = \lambda_3 = 1$. This leads to the Lie algebra of $\mathbb{S}^3$, and does not produce any new geometry.

$\lambda_1 = \lambda_2 = -\lambda_3 = 1$. This gives the Lie algebra of the previously found $\mathbb{S}^2 \times \mathbb{R}$ geometry, nothing new either.

$\lambda_1 = 1$, $\lambda_2 = \lambda_3 = 0$. This gives the Heisenberg group, which was seen to correspond to Nil geometry.

$\lambda_1 = \lambda_2 = \lambda_3 = 0$. This is of course the well known $\mathbb{E}^3$ case, which has also previously been encountered.

$\lambda_1 = 1$, $\lambda_2 = 0$, $\lambda_3 = -1$. This combination of structure constants produces no geometry.

2.3.1 Sol

The last possibility and the only one leading to a new and valid geometry is $\lambda_1 = \lambda_2 = 1$, $\lambda_3 = 0$. The geometry thus formed is called solve geometry. $\lambda_3 = 0$ essentially means that e_1 and e_2 commute. Therefore e_1 and e_2 must be acting on some copy of $\mathbb{R}^2$ as a subgroup of the Lie group. The quotient must be $\mathbb{R}$, so that the Lie group must be $\mathbb{R}^2 \rtimes \mathbb{R}$.

3 The Poincaré Dodecahedral Space

As suggested when first introduced, the PDS is a 3-manifold, admitting a geometry modelled on the 3 sphere. This means that there is some group of isometries of S^3, $I^* < O(4)$, such that PDS $\cong S^3/I^*$, which was called the binary icosahedral group. This binary icosahedral group, I^* was the preimage of the icosahedral group under the 2:1 $SU(2) \to SO(3)$ homomorphism. This group is finite and therefore properly discontinuous and also acts freely, so indeed S^3/I^* is a well-defined spherical manifold. Since the homomorphism along which the icosahedral group is pulled back is 2:1, $\#I^* = 2\#I$. Since $\#I = 20 * 3 = 60$, this means $\#I^* = 120$.

The course of action taken in the remainder of this section will be to show that there must be a tessellation of S^3 by fundamental cells of S^3/I^*. Once this is established, the number of possible fundamental cells will be systematically reduced until only four are left. At this point, an upper bound will be set for the number of cells in a tessellation by each of the fundamental cells, at which point only one tessellation remains possible.

The first thing to notice, though, is that $I^* \not\cong C_{120}$, which is left as an exercise to the reader. Therefore, the degenerate case of a lens space can be dismissed, and the fundamental cells are truly polyhedra.

3.1 Voronoi cells

Consider picking an arbitrary point e on S^3, and consider its orbit O under T. Any point in O can be written uniquely as te, since if $te = se$, $e = t^{-1}se$, which since T acts freely implies $t^{-1}s = 1$ or $t = s$. So acting on e provides a bijection between T and O, where $1 \mapsto e$. This fact will be utilised by writing $\hat{p}$ for the unique element in T carrying e to p.

Definition 6. $V_p = \left\{ x \in S^3 \middle| \forall q \in O : \mathrm{d}(x,p) \le \mathrm{d}(x,q) \right\}$ is called the *Voronoi cell* of p.

Lemma 1. *The Voronoi cells of some finite $O \subset S^3$ tessellate S^3. Also, these Voronoi cells are convex polyhedra and in the case that O is the orbit of a single point under a group of isometries, all Voronoi cells are congruent.*

Proof. Since every point in S^3 has at least one nearest neighbour in O, $\bigcup_{p \in O} V_p = S^3$. Furthermore, $V_p \cap V_q \subset \left\{ x \in S^3 \middle| \mathrm{d}(x,p) = \mathrm{d}(x,q) \right\}$, which is a plane. So the intersections of two cells is at most a face, as it should be in a tessellation. This proves that the Voronoi cells provide a tessellation for S^3. Notice that $\left\{ x \in S^3 \middle| \mathrm{d}(x,p) \le \mathrm{d}(x,q) \right\}$ is a half-space and a Voronoi cell can be viewed as a finite (since O is finite) intersection of such sets. Thus, the Voronoi cells are convex polyhedra.

$$
\begin{aligned}
V_p &= \left\{ x \in S^3 \,\middle|\, \forall q \in O : \mathrm{d}(x,p) \leq \mathrm{d}(x,q) \right\} \\
&= \left\{ x \in S^3 \,\middle|\, \forall \hat{p}^{-1}q \in \hat{p}^{-1}O : \mathrm{d}(x,p) \leq \mathrm{d}(x,\hat{p}\hat{p}^{-1}q) \right\} \\
&= \left\{ x \in S^3 \,\middle|\, \forall r \in O : \mathrm{d}(x,\hat{p}e) \leq \mathrm{d}(x,\hat{p}r) \right\} \\
&= \left\{ \hat{p}x \in \hat{p}S^3 \,\middle|\, \forall r \in O : \mathrm{d}(\hat{p}x,\hat{p}e) \leq \mathrm{d}(\hat{p}x,\hat{p}r) \right\} \\
&= \left\{ \hat{p}x \in S^3 \,\middle|\, \forall r \in O : \mathrm{d}(x,e) \leq \mathrm{d}(x,r) \right\} \\
&= \hat{p}V_e
\end{aligned}
$$

Since $\hat{p} \in T < \mathrm{O}(4)$ implies $\hat{p}^{-1}O = O$, $\hat{p}S^3 = S^3$, and $\mathrm{d}(\hat{p}x,\hat{p}y) = \mathrm{d}(x,y)$. This means that all Voronoi cells are congruent to V_e, and thus congruent to each other. $\qquad\square$

So, now we have a tessellation of S^3 by congruent convex polyhedra. S^3/I^* is exactly one such polyhedron, but with its faces identified accordingly. Left to show is, that these polyhedra are indeed regular dodecahedra. Opposing faces of such a dodecahedron should also be identified with a minimal twist of $\frac{\pi}{5}$.

3.2 Topological constraints

Not all regular polyhedra can be used to tile S^3. Firstly, some topological considerations.

Definition 7. When a small sphere is taken around a vertex of the tessellation, the intersection of the sphere and an edges becomes a point on the sphere and the intersection of the sphere and a face becomes a geodesic on the sphere. Replacing these geodesics between points are by straight lines through the same endpoints results in a regular polyhedron called a *vertex figure*.

Lemma 2. *There are exactly 11 tessellations of regular polyhedra:*

- *A tessellation by tetrahedra, cubes, or dodecahedra with tetrahedral, octahedral, or icosahedral vertex figures.*

- *A tessellation by octahedra with cubic vertex figures.*

- *a tessellation by icosahedra, with dodecahedral vertex figures.*

Proof. It is easily seen, and was so by Euler, that if we call the number of vertices of such a tiling V, the number of edges E, the number of faces F and the number of cells C, we must have $V - E + F - C = 0$. Call the number of vertices of each cell V_C, the number of cells that intersect in one vertex C_V, and likewise for edges and faces. We have symbolically $XY_X = YX_Y$ for $X,Y \in \{V,E,F,C\}$, thus:

$$
\begin{aligned}
0 &= V - E + F - C \\
&= C\left(\frac{V_C}{C_V} - \frac{E_C}{C_E} + \frac{F_C}{C_F} - 1 \right) \\
1 &= \frac{V_C}{C_V} - \frac{E_C}{C_E} - \frac{F_C}{C_F}
\end{aligned}
$$

11

But, surely each face is shared by 2 cells, so $C_F = 2$, and within one cell we have $V_C - E_C + F_C = 2$, so $F_C - 2 = E_C - V_C$. Define $Q = 2\frac{E_C}{V_C}$, which is the number of edges joining in each vertex in a single cell. Note that this is always larger than 2, so that $Q - 2$ can never be zero.

$$
\begin{aligned}
1 &= \frac{V_C}{C_V} - \frac{E_C}{C_E} + \frac{F_C}{C_F} \\
0 &= \frac{V_C}{C_V} - \frac{E_C}{C_E} + \frac{F_C - 2}{2} \\
&= \frac{V_C}{C_V} - \frac{E_C}{C_E} + \frac{E_C - V_C}{2} \\
&= V_C \left(\frac{1}{C_V} - \frac{Q}{2C_E} + \frac{Q-2}{4} \right) \\
0 &= \frac{1}{C_V} - \frac{Q}{2C_E} + \frac{Q-2}{4} \\
&= \frac{Q-2}{4C_V C_E} \left(\frac{4}{Q-2}C_E - \frac{2Q}{Q-2}C_V + C_V C_E \right) \\
0 &= \frac{4}{Q-2}C_E - \frac{2Q}{Q-2}C_V + C_V C_E \\
&= -\left(\frac{4}{Q-2} + C_V \right)\left(\frac{2Q}{Q-2} - C_E \right) + \frac{8Q}{(Q-2)^2}
\end{aligned}
$$

So ultimately:

$$
\left(\frac{4}{Q-2} + C_V \right)\left(\frac{2Q}{Q-2} - C_E \right) = \frac{8Q}{(Q-2)^2} \tag{1}
$$

The tetrahedron, cube, and dodecahedron all have $Q = 3$. The octahedron has $Q = 4$, and the icosahedron has $Q = 5$. For $Q = 3$, equation 1 becomes:

$$
(4 + C_V)(6 - C_E) = 24
$$

C_V and C_E must always be greater than 2 to get a genuine polychoron. This leaves $24 = 8 \cdot 3 = 12 \cdot 2 = 24 \cdot 1$, leading to $(C_V, C_E) = (4,3), (8,4), (20,5)$ respectively. For $Q = 4$, equation 1 becomes:

$$
(2 + C_V)(4 - C_E) = 8
$$

Leaving $8 = 8 \cdot 1$, corresponding to $(C_V, C_E) = (6,3)$ Finally, for $Q = 5$, equation 1 becomes:

$$
\left(\frac{4}{3} + C_V \right)\left(\frac{10}{3} - C_E \right) = \frac{40}{9}
$$

which is more conveniently written as:

$$
(4 + 3C_V)(10 - 3C_E) = 40
$$

With only solution $40 = 40 \cdot 1$, meaning $(C_V, C_E) = (12, 3)$.

These combinatorial properties provide some information about the vertex figures. The vertex figures of a tessellation with (C_V, C_E), will have C_V faces and C_E faces per vertex. So, what has in fact been established through topological means, is that tetrahedral, cubic, and dodecahedral tessellations have tetrahedral, octahedral, or icosahedral vertex figures. Octahedral tessellations will have cubic vertex figures, and an icosahedral tessellation will have dodecahedral vertex figures. □

3.3 Geometrical constraints

Not all of these tessellations are tessellations of S^3, some might tile euclidean or even hyperbolic space. The dihedral angle of spherical polyhedron is always greater than the dihedral angle of their euclidean equivalent, which in turn is greater than a hyperbolic one. To see which are spherical, we can therefore calculate the dihedral angle, which is $\frac{2\pi}{C_E}$.

Lemma 3. *Of the 11 topological tessellations from section 3.2, the following correspond to the following spaces:*

	Cells	Vertex figures
Spherical:	Tetrahedral	Tetrahedral
	Tetrahedral	Octahedral
	Tetrahedral	Icosahedral
	Cubic	Tetrahedral
	Dodecahedral	Tetrahedral
	Octahedral	Cubic
Euclidean:	Cubic	Octahedral
Hyperbolic:	Cubic	Icosahedral
	Dodecahedral	Cubic
	Dodecahedral	Icosahedral
	Icosahedral	Dodecahedral

Proof. Euclidean tetrahedra have a dihedral angle of $\arccos\left(\frac{1}{3}\right) \approx 1.231$, which is smaller than $\frac{2\pi}{C_E}$ for $C_E = 3, 4, 5$. So all tetrahedral tessellations, having tetrahedral, octahedral, or icosahedral vertex figures, tile S^3.

Euclidean cubes have a dihedral angle of $\frac{\pi}{2}$, which is equal to $\frac{2\pi}{C_E}$ for $C_E = 4$. So the cubic tessellation having tetrahedral vertex figures tiles S^3. The cubic tessellation having octahedral vertex figures tiles $\mathbb{R}^3$. And the cubic tessellation having icosahedral vertex figures can only tile $\mathbb{H}^3$.

Euclidean dodecahedra have a dihedral angle of $\arccos\left(-\frac{1}{5}\sqrt{5}\right) \approx 2.034$, which is smaller than $\frac{2\pi}{C_E}$ only for $C_E = 3$, and larger than $\frac{2\pi}{C_E}$ for $C_E = 4, 5$. So, like the cubic tessellation, the dodecahedral tessellation with tetrahedral vertex figures tiles S^3. The dodecahedral tessellations with octahedral or icosahedral vertex figures tile $\mathbb{H}^3$.

Euclidean octahedra have a dihedral angle of $\arccos\left(-\frac{1}{3}\right) \approx 1.911$, which is smaller than $\frac{2\pi}{3}$. This means that the only octahedral tessellation, with cubic vertex figures, tiles S^3.

Euclidean icosahedra have a dihedral angle of $\arccos\left(-\frac{1}{3}\sqrt{5}\right) \approx 2.412$, which is larger than $\frac{2\pi}{3}$. So the only icosahedral tessellation, with dodecahedral vertex figures, tiles $\mathbb{H}^3$. $\qquad\square$

3.4 Symmetry constraints

Not all of these tilings can be constructed as the orbit of a fundamental domain under some $I^* < \mathrm{O}(4)$.

Lemma 4. *$I^* < \mathrm{O}(4)$, and P some polyhedron such that the orbit of P under I^* tessellates some space. Then this tessellation has $C_F | F_C$, $C_E | E_C$, and $C_V | V_C$.*

Proof. If this is to be the case, then the different cells in the tessellation can be identified as can their faces, edges, and vertices. Choose a cell and a face, edge, or vertex on this cell shared by C_F, C_E, or C_V cells respectively. Under I^*, this face, edge, or vertex will be equivalent to another face, edge, or vertex in all of the other cells sharing it. In one fundamental cell, all these different images of one face, edge, or vertex are identified, creating equivalence classes of C_F, C_E, or C_V elements respectively. So the number of faces, edges, or vertices, F_C, E_C, or V_C, must be divisible by C_F, C_E, or C_V. $\qquad\square$

The result that $C_F | F_C$ does not contribute anything, however since $C_F = 2$, and $2 | F_C$ for all regular polyhedra. The results that $C_E | E_C$ and $C_V | V_C$ do contribute, though their contributions are the same.

Corollary 4.1. *Of the 11 tessellations of section 3.2, the following four are not the orbit of a cell under some group:*

- *The tetrahedral tessellation with octahedral vertex figures*

- *The tetrahedral tessellation with icosahedral vertex figures*

- *The cubic tessellation with icosahedral vertex figures*

- *The dodecahedral tessellation with octahedral vertex figures*

Proof. Tetrahedra have $(E_C, V_C) = (6, 4)$, so the octahedral and icosahedral vertex figures, leading to $(C_E, C_V) = (4, 8), (5, 20)$ can by lemma 4 not lead to a tessellation, which is the orbit of some group.

Cubes have $(E_C, V_C) = (12, 8)$, so the icosahedral vertex figure, leading to $(C_E, C_V) = (5, 20)$ cannot produce a valid tessellation.

Dodecahedra have $(E_C, V_C) = (30, 20)$, so octahedral vertex figures, leading to $(C_E, C_V) = (4, 8)$ cannot produce a valid tessellation as well. $\qquad\square$

3.5 Cell counting

At this point there are four tessellations left which are both spherical and the orbit of a group. Further reduction of the number of possible tessellations seems possible nor necessary. The only bit of information left unused is that

$C = \#I^* = 120$, so the next step to take is to calculate the number of cells in each of these tessellations. To accomplish this, one has to calculate the volume of one cell and compare it to the volume of S^3, which is $2\pi^2$ in units of the radius of curvature. Calculating the volume of a spherical polyhedron is rather tedious, though, so instead the area will be calculated. The area will then be used to estimate the volume of the cell, and as it turns out, a lower bound can be found.

The dihedral angles, which we will call θ_d of the fundamental polyhedra of a tiling of space are very straightforward to determine. Since a closed loop around any edge should represent a total angle of 2π, the dihedral angle of 1 of the C_E cells meeting there should be $\frac{2\pi}{C_E}$. To calculate the area of a face of a spherical polyhedron, we needs the angles between meeting edges in the face, call these θ_f, or face angles.

The face angle of a spherical polyhedron should be completely determined by the dihedral angle. To find the dependence we consider the tangent space to S^3 in a vertex of the polyhedron. The different edges meeting in the vertex can now be identified with their (one-sided) derivatives in the vertex. The angles between the tangent vectors will by definition give the angle between the edges. It should be clear that the set of these tangent vectors is closed under rotations of $\frac{2\pi}{Q}$ around the direction given by their sum. Thus, these vectors must form a Q-gonal pyramid, where the height of the pyramid is related to the curvature of the ambient space containing the polyhedron in question.

To our great fortune, only two different values of C_E remain possible for any quotient like tessellation of S^3. These values are as mentioned before 3 and 4, so for the sake of definiteness, assume $Q = 3$.
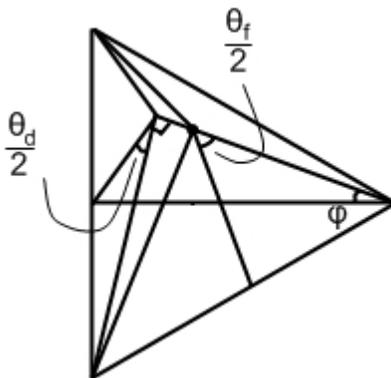
Figure 1: Construction for the determination of the functional relationship between θ_d and θ_f in a triangular pyramid

Q=3 If $Q = 3$, a triangular pyramid must be considered, which is depicted in figure 1. Since the goal of our endeavour concerns solely angles, the scale is

free to choose. For convenience, I have chosen the distance between any two non-top vertices of the pyramid to be $\sqrt{3}$. Figure 1 shows clearly that

$$\sin(\phi) = \frac{\frac{1}{2}\sqrt{3}\cot\left(\frac{\theta_d}{2}\right)}{\frac{3}{2}} = \frac{1}{3}\sqrt{3}\cot\left(\frac{\theta_d}{2}\right)$$

as well as

$$\cos(\phi) = \frac{1}{\frac{1}{2}\sqrt{3}\csc\left(\frac{\theta_f}{2}\right)} = \frac{2}{3}\sqrt{3}\sin\left(\frac{\theta_f}{2}\right)$$

The elaborate fractions in between the equality signs are meant to guide the reader as to which triangles should be considered to arrive at these expressions. These expressions can be combined using the famous identity $\cos^2(\theta)+\sin^2(\theta) = 1$, which will eliminate φ, to obtain the following.

$$1 = \left(\frac{1}{3}\sqrt{3}\cot\left(\frac{\theta_d}{2}\right)\right)^2 + \left(\frac{2}{3}\sqrt{3}\sin\left(\frac{\theta_f}{2}\right)\right)^2 = \frac{1}{3}\cot^2\left(\frac{\theta_d}{2}\right) + \frac{4}{3}\sin^2\left(\frac{\theta_f}{2}\right)$$

To make this expression even more appealing to the eye and easier to evaluate, I will use some slightly more obscure trigonometric identities, which can easily be confirmed using the complex form of sin and cos. First of these identities is $2\sin^2\left(\frac{\theta}{2}\right) = 1 - \cos(\theta)$ and the second is $\cot^2\left(\frac{\theta}{2}\right) = \frac{1+\cos(\theta)}{1-\cos(\theta)}$.

$$
\begin{aligned}
1 &= \frac{1}{3}\cot^2\left(\frac{\theta_d}{2}\right) + \frac{4}{3}\sin^2\left(\frac{\theta_f}{2}\right) \\
&= \frac{1}{3}\frac{1+\cos(\theta_d)}{1-\cos(\theta_d)} + \frac{2}{3}\left(1 - \cos(\theta_f)\right) \\
\cos(\theta_f) &= 1 - \frac{1}{2}\left(3 - \frac{1+\cos(\theta_d)}{1-\cos(\theta_d)}\right)
\end{aligned}
$$

So for a $Q = 3$ tiling of S^3, we have obtained the following relation between the dihedral and face angles.

$$\cos(\theta_f) = \frac{\cos(\theta_d)}{1 - \cos(\theta_d)} \tag{2}$$

Q=4 If $Q = 4$, a square pyramid is to be considered, which is depicted in figure 2. For convenience, choose the sides of the base square to be of length 2. Then it should be clear from figure 2, that

$$\cos(\phi) = \frac{\sqrt{2}}{\csc\left(\frac{\theta_f}{2}\right)} = \sqrt{2}\sin\left(\frac{\theta_f}{2}\right)$$

As opposed to the approach used in the $Q = 3$ case, we now use another construction to determine the functional relation between φ and θ_d. The figure associated with this approach is figure 3, where the horizontal and vertical line

16
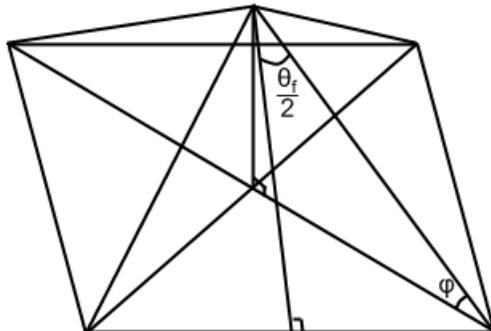
Figure 2: Construction for the determination of the functional relationship between θ_f and φ in a square pyramid

contain sides of the square that is the base of the pyramid. The scale of the picture is not really relevant, as long as it is clear that the lines denoted by perpendicular strokes share a single length, say 1. Due to this relative small dependence on the actual pyramid it might not be entirely clear why the angle denoted as θ_d is in fact θ_d. This is the case however, since it is an angle between lines on a face (since their endpoints are), perpendicular to the edge in which they meet. With this knowledge it is easily seen that

$$\sin(\varphi) = \cot\left(\frac{\theta_d}{2}\right)$$

The remaining procedure is entirely equivalent to the $Q = 3$ case, so I will allow myself to skip some of the intermediate steps this time.

$$
\begin{aligned}
1 &= \cot^2\left(\frac{\theta_d}{2}\right) + 2\sin^2\left(\frac{\theta_f}{2}\right) \\
&= \frac{1 + \cos(\theta_d)}{1 - \cos(\theta_d)} + 1 - \cos(\theta_f)
\end{aligned}
$$

So for a $Q = 4$ tiling of S^3 we have obtained the following relation for the face angle as a function of the dihedral angle.

$$\cos(\theta_f) = \frac{1 + \cos(\theta_d)}{1 - \cos(\theta_d)} \tag{3}$$

Equations 2 and 3 allow us to determine the face angle of the fundamental cell of a tiling of S^3, but the real information sought is the volume of such a cell. Since deriving the second from the first seems to require very painstaking calculations, another approach will be taken. Remarkably, the area of a spherical polygon can be determined from its face angles with great ease. A spherical triangle on the sphere with radius 1 and with the sum of its angles being Σ_θ,

17
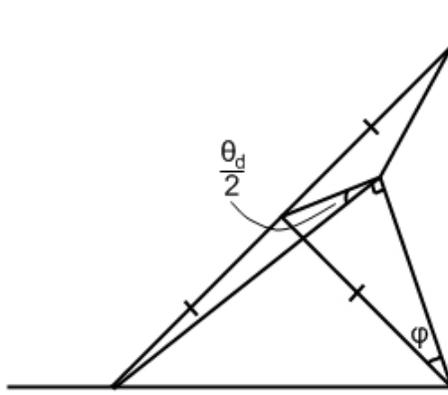
Figure 3: Construction for the determination of the functional relationship between θ_d and φ in a square pyramid

will have an area of exactly $\Sigma_\theta - \pi$. Any spherical n-gon, with angle sum Σ_θ on the same sphere can be considered a union of $n-2$ triangles. The angle sums of these individual triangles are unknown but the sum of their angle sums should equal Σ_θ. Therefore the total area of such an n-gon should be $\Sigma_\theta - (n-2)\pi$, or somewhat more nicely, employing some abuse of notation $2\pi - \Sigma_{\pi-\theta}$.

If S^3 is imagined to be embedded in $\mathbb{R}^4$, the faces, being geodesic planes, are in fact intersections of S^3 with $\mathbb{R}^4$ subspaces. Such an intersection is an embedding of S^2, and since these euclidean subspaces contain the origin, these S^2 are in fact of the same radius as the original S^3.

If we are to evaluate the area of a polyhedron, we should have a convention as to which units to use. For the sake of simplicity, I will define the radius of curvature of the ambient space S^3 to be 1. Using the argument just given, this means that the faces of a fundamental cell lie on a sphere of radius one, which using the previous argument means that their area is given by $2\pi - \Sigma_{\pi-\theta}$. The θ here are of course just the θ_f, that have painstakingly been calculated. Due to the symmetry of the faces in their vertices and the polyhedron in its faces, the total area of the entire polyhedron is given by

$$A = F_C \left(2\pi - V_F(\pi - \theta_f)\right) \tag{4}$$

Where θ_f is to be determined from $\theta_d = \frac{2\pi}{C_E}$ by equation 2 or 3.

The calculation of the area of a fundamental cell is thus completely solved now, but this was not really the question at hand. Luckily we are but one observation away from an estimate of what we set out to calculate. The observation to be made is that a spherical polyhedron of area A has volume V at least as large as the volume of the corresponding euclidean polyhedron of area A. The effect is actually twofold, since as the curvature increases, not only will the boundary resemble a sphere more and more, but also the interior will be-

come increasingly displaced from the euclidean 3-space containing the vertices, effectively gaining volume in the fourth euclidean dimension.

At this point all the tools are in place to produce lower boundaries to the volume of a spherical polyhedron based on its dihedral angle. A lower boundary for volume is equivalent to an upper boundary for number of cells, since $V \cdot C = 2\pi^2$, the volume of S^3 (with radius of curvature 1).

Tetrahedron   The first of the geometrically possible tessellations of S^3 was a tetrahedral tiling with tetrahedra as vertex figures. Tetrahedra, as the vertex figure have $Q = 3$, so $C_E = 3$ and $\theta_d = \frac{2}{3}\pi$. In fact the only geometrically possible vertex figures, the tetrahedron and the cube, both have $Q = 3$, so $\theta_d = \frac{2}{3}\pi$ for all other tessellations as well. Since tetrahedra are also the cells, the cell-Q is also 3 and equation 2 has to be used to obtain θ_f.

$$\cos(\theta_f) = \frac{\cos\left(\frac{2}{3}\pi\right)}{1 - \cos\left(\frac{2}{3}\pi\right)} = -\frac{1}{3}$$

Since $\cos(\pi - \theta) = -\cos(\theta)$, $\pi - \theta = \arccos\left(\frac{1}{3}\right)$ and using equation 4

$$A = 8\pi - 12\arccos\left(\frac{1}{3}\right) > 10.361$$

For a euclidean tetrahedron $V^2 = \frac{\sqrt{3}}{648}A^3$, so $V \geq \sqrt{\frac{\sqrt{3}}{648}A^3} > 1.724$ and finally for a tetrahedral tiling.

$$C = \frac{2\pi^2}{V} < \frac{2\pi^2}{1.724} < 12$$

Cube   Another geometrically possible tessellation is one by cubes, with tetrahedra as vertex figure. As stated $\theta_d = \frac{2}{3}\pi$, and since cubes also have $Q = 3$, equation 2 has to be used again. The same equation with the same θ_d, means that again $\pi - \theta_f = \arccos\left(\frac{1}{3}\right)$. This time the area becomes

$$A = 12\pi - 24\arccos\left(\frac{1}{3}\right) > 8.156$$

For a euclidean cube $V^2 = \frac{1}{216}A^3$, so $V \geq \sqrt{\frac{1}{216}A^3} > 1.584$ and finally for a cubic tiling of S^3.

$$C = \frac{2\pi^2}{V} < \frac{2\pi^2}{1.584} < 13$$

Dodecahedron   The third possible tessellation of S^3 is the tessellation by dodecahedra called the PDS. Like the previous two possibilities, the PDS also has tetrahedra for vertex figures. Also, like the previous cases the dodecahedron has $Q = 3$, so again equation 2 should be used, leading to $\pi - \theta_f = \arccos\left(\frac{1}{3}\right)$. The area becomes

$$A = 24\pi - 60\arccos\left(\frac{1}{3}\right) > 1.540$$

For a euclidean dodecahedron $V^2 = \frac{\left(15+7\sqrt{5}\right)^2}{432\sqrt{25+10\sqrt{5}}^3}A^3 > \frac{2669}{400000}A^3$, so $V > \sqrt{\frac{2669}{400000}A^3} > 0.156$ and finally for a dodecahedral tiling of S^3.

$$C = \frac{2\pi^2}{V} < \frac{2\pi^2}{0.156} < 127$$

Octahedron The last tessellation of S^3 under consideration is the tessellation by octahedra with cubical vertex figures. In this case, although the cube has $Q = 3$, and therefore $\theta_d = \frac{2}{3}\pi$, the octahedron has $Q = 4$ and thus equation 3 must be used. The result of this is that

$$\cos(\theta_f) = \frac{1 + \cos\left(\frac{2}{3}\pi\right)}{1 - \cos\left(\frac{2}{3}\pi\right)} = \frac{1}{3}$$

Differing exactly a sign with the $Q = 3$ case. The total area is still provided by equation 4, and turns out to be

$$A = 24\arccos\left(\frac{1}{3}\right) - 8\pi > 4.410$$

For a euclidean octahedron $V^2 = \frac{\sqrt{3}}{324}A^3$, so $V \geq \sqrt{\frac{\sqrt{3}}{324}A^3} > 0.677$ and finally, the octahedral tiling of S^3 has.

$$C = \frac{2\pi^2}{V} < \frac{2\pi^2}{0.677} < 30$$

3.6   Conclusion

Combining the results of the previous subsections, it has been shown that there might exist 4 tessellations of S^3 by regular polyhedra, of which only one could have 120 elements. The space S^3/I^* must therefore be equal to the space resulting from identifying the sides of a fundamental cell of this tessellation, a dodecahedron. There are in fact two ways to identify faces of a polyhedron, one can identify opposite sides with a $\frac{1}{5}\pi$ twist, or with a $\frac{3}{5}\pi$ twist. The resulting spaces are shown in figure 4 and 5 respectively.

   To see which one corresponds to the PDS, one counts C_E. Firstly, count C_E for the minimal twist space, seen in figure 4. Start one the centre face A near side 15 and walking through the dodecahedron towards face D side 34. 1 dodecahedron has now been traversed and one can pass through the identification to the other side D. Here, traversing the dodecahedron leads to face B side 15, two dodecahedra have now been traversed. Again passing through the identification to the other side B, one can once more traverse the dodecahedron leading to face A side 15. 3 dodecahedra have now been traversed and if one passes through the identification once more, one arrives at the starting point. So a loop around the A15 edge in the minimal twist space taken one through 3 dodecahedra, meaning that for this space $C_E = 3$.
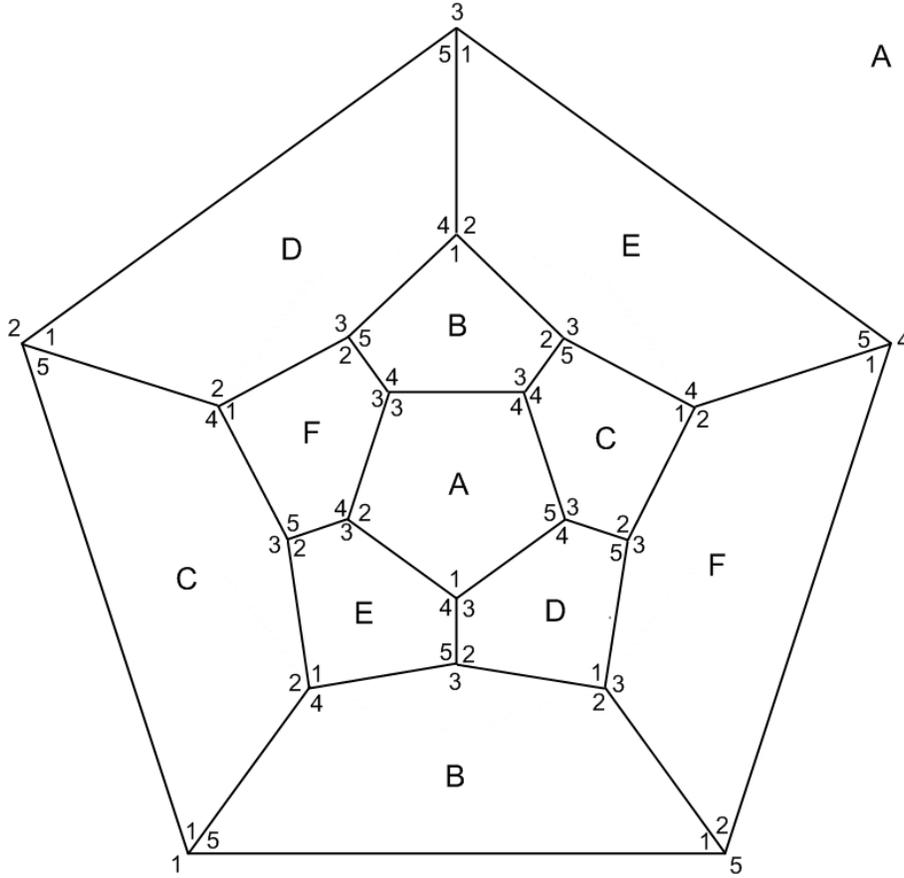
Figure 4: Schlegel diagram of the dodecahedron with sides identified with minimal twist

For the maximal twist space, seen in figure 5, again start near A15. Traversing the first dodecahedron again takes one near D34. Using the identification, one arrives in the other D34, and traversing the second dodecahedron takes one to E15. The identification is used and the third dodecahedron is traversed leading to B23. Once more, one can use the identification to travel through the fourth dodecahedron leading to C45. After using the identification, finally the fifth dodecahedron is traversed leading to A15, which after one more identification takes one to the starting point. So in the maximal twist space, a small loop around the A15 side takes one through 5 different dodecahedra, meaning $C_E = 5$.

As was seen in section 3.3 this means that the minimal twist space is a spherical dodecahedral space with tetrahedral vertex figures and the maximal
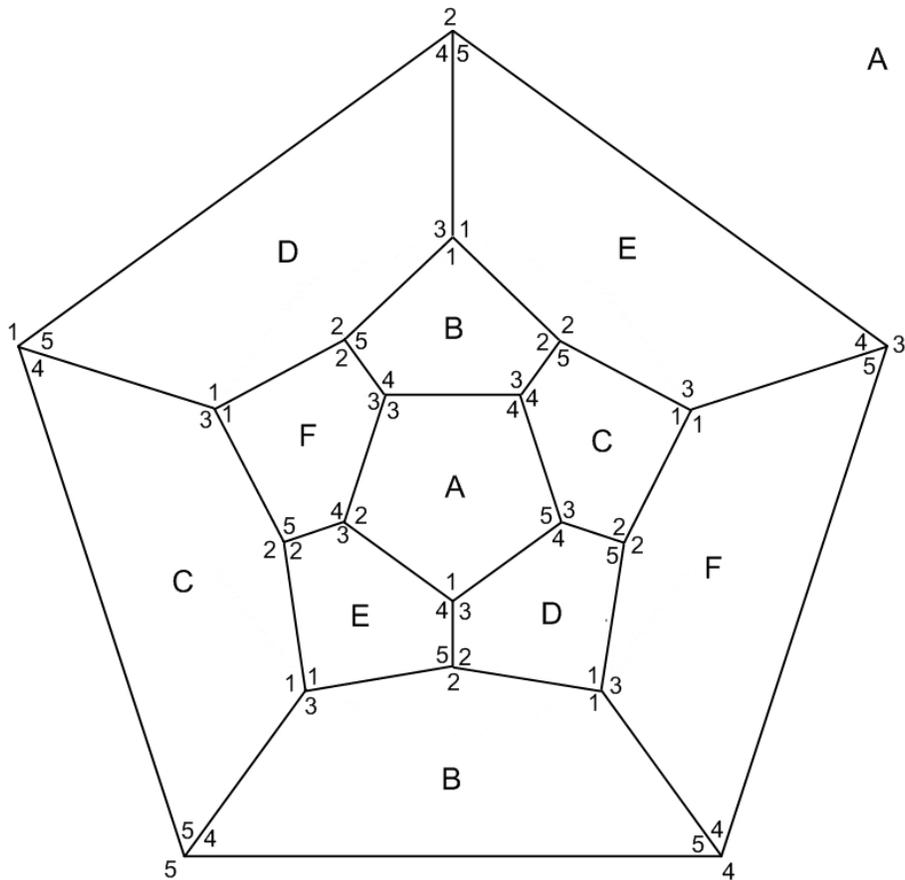
Figure 5: Schlegel diagram of the dodecahedron with sides identified with maximal twist

twist space is thus a hyperbolic dodecahedral space with icosahedral vertex figures. Using this information it is clear that the spherical PDS must be the minimal twist space, that is, the space obtained by identifying the opposite sides of a dodecahedron with a twist of $\frac{1}{5}\pi$.

4 Physical Topological Phenomena

As promised, this section will explore some of the physical consequences of non-simply connected spherical space in general and especially the PDS as a model for our universe. Before this is attended to, some explanation may be in place regarding the credibility of the model. The first apparent mistake in the claims made by this article concerns the dimension of the model used. After all, since the subject of cosmology is so intimately connected to general relativity, especially in the non-flat case, space-time should be considered in its entirety, leaving us to model a 4-dimensional manifold instead of a 3-dimensional one, such as the PDS. Fortunately, the universe is as usual stranger and more kind than naïvely suspected, providing us with what is known as Weyl's principle[8].

Theorem 5. *The world lines of galaxies, or 'fundamental particles', form (on average) a spacetime-filling family of non-intersecting geodesics converging towards the past.*

What Weyl is asserting here is that the world lines of the universe, basically the geodesics, foliate it, at least if we forget about the initial singularity. This means, that the time of an event may be defined to be the proper time on the unique world line containing it. We can now define the spatial part of the universe at some time t to be the collection of events with that time associated to it by the previous method. By hypothesis and smooth dependence on initial conditions, this will provide us with a smooth 3-dimensional manifold associated with each time. By continuous dependence on initial conditions, time-evolution as well as time-devolution, being essentially the same thing, by some fixed time τ is a continuous operation. Thus, geodesic time-evolution provides homeomorphisms between the universe at any time, meaning that its topology is constant in time. So, in conclusion the space-time manifold can on cosmic scales be interpreted as a product space of a 1-dimensional time line and a 3-dimensional "space"-space, it is of course this latter space in which we are really interested.

The first thing we assume now, is homogeneity of space. This is by no means a reasonable assumption, although it is backed by some empirical evidence. Physical theories certainly seem to be invariant under spatial translations, in fact this is equivalent to conservation of momentum, which is one of the pillars of modern physics and extremely well tested as such. Although this is a clear indication of the homogeneity, it is not proof. In fact, most of this section has so far been dedicated to proving that a theoretical invariance can be broken by reality. Regrettably, since we can only directly observe our immediate surroundings, our hand is forced in this matter and we will have to accept spatial homogeneity for its symmetry if we are to say anything about space as a whole.

Another assumption that is canonically made in cosmology is isotropy. Since homogeneous spaces are fairly limited in number, the additional assumption of isotropy is not strictly necessary. Isotropy is, however, in contrast to homogeneity, quite convincingly confirmed. Therefore, and because it will simplify matters considerably, the universe will at least be considered locally isotropic. Local isotropy is understood here to imply geometric isotropy, but not neces-

sarily topological isotropy. From the considerations in section 2 it is clear that there are 8 different homogeneous 3-dimensional geometries of which exactly 3 are isotropic. These three geometries are of course exactly the ones singled out by the Friedman-Robertson-Walker metric. In contrast to the models accounted for by this metric, the topology of our model will *not* be assumed simply connected leaving us with some additional possible spaces to consider.

With the assumptions in place, now is the time to start considering how to eliminate possibilities based on empirical evidence. Since there are three geometries left, all representing many manifolds, the nicest thing to do would be to try and eliminate one or two geometries. Conveniently, Einstein provided the world with a theory describing exactly the geometry of space as a function of its energy content. As it turns out, under the assumption of isotropy and homogeneity, the geometry of the universe is governed by a single parameter, the curvature, which is completely governed by the mean energy density. A constant $\Omega = \frac{\rho}{\rho_c}$ is customarily defined, where ρ is the energy density and ρ_c is the energy density needed for space to be exactly flat. This way $\Omega = 1$, clearly indicates a flat space, whereas $\Omega > 1$ means that an abundance of energy will contract space, giving it spherical geometry, finally $\Omega < 1$ occurs in very low-energy space leaving it hyperbolic in its geometry.

Considerable effort has of course been put in trying to determine the value of Ω. Currently $\Omega = 1.005 \pm 0.006$, sadly not even eliminating one of the three geometries, although hyperbolic geometry should be considered unlikely. For the sake of the argument, the flat case is discarded for now. If one considers the energy content of the universe to forego its curvature, which is a highly metaphysical and perhaps rather dubious claim, this case very unlikely anyway.

The first observation the reader will have made, is that any manifold, admitting the empirically favoured spherical geometry, is bounded. In this scenario, there is certainly a possibility that by a stroke of good fortune we find ourselves in a universe smaller than our horizon. If this is indeed the case, we ought to be able to detect it. A number of ways to do so have been conceived, and I will treat all of which I am aware.

4.1 Searching for duplicates

When one suspects to be in a hall of mirrors, a natural cause of action would be to search for one's mirror images. Sadly a cosmic mirror image is very hard to find. The first problem one encounters in this course of action is the fact that we, and therefore our mirror images, are quite small compared even to a plausible finite universe. In addition to this, there is no preferred way to look, so the whole operation would be something of a needle in a haystack search. Additional complications stem from the fact that our images might be considerably obscured by other celestial bodies, or intergalactic gas. To complicate things even further we don't know from which angle we would view ourselves, nor do we know the distance to these images we would be looking for. This last problem is not much of a problem in an actual hall of mirrors, but on cosmic scales space separation means time separation due to the finite speed of

light. So what we are looking for is a picture of ourselves from any angle, from any time in the distant past, anywhere in a universe full of noise.

The problem is twofold: not only don't we know where to look and if our image is even visible to us, but we probably wouldn't even be able to recognize our picture if we saw it.

4.2   Circles in the sky

Another approach would be to search for other objects occurring twice within the visible universe. This largely has the same problems as the search for mirror images, except for the fact that in this way, one would only hav to look half as far, effectively reducing the curvature by a factor of two. The approach can be generalized in another way, though, by realizing that it is not really double objects we're looking for, but double space. This means that any phenomenon occurring in space can be used to search for "duplicates". In particular the CMB might be used. The CMB is far easier to detect than actual objects, especially since it's time-evolution is far more predictable. The disadvantage here is that the CMB is fairly homogeneous, so only the fluctuations, which have a relative magnitude of about 1 in 10^5, can really be used.

If our visible universe were exactly as big as a fundamental domain of space, we would see equal points in different directions on our horizon. If the universe is any older or smaller, a somewhat more complicated situation occurs, where the sphere making up our horizon crosses a face of the fundamental domain. Wherever these intersections occur, they do so from both sides, and therefore define events observed simultaneously from two directions. The faces of the fundamental domain are sections of spheres, so the intersection with the horizon will consist of diametrically opposed circles.[2]

Hence, another test for multiply-connected space models is to search for diametrically opposed equal circles, which due to random noise should in reality be a search for correlated diametrically opposed circles. Searches for these "circles in the sky" have been proposed in since 1996 and have been used to test the PDS model at least since 2003[5]. In 2003 the method found no correlated diametrically opposed circles, but the correlations sought for were only in unturned circles. As seen in section 3 the PDS space has neighbouring copies differ by a twist of 36° along the common axis. Even when these relative rotations were taken into account no correlations were found, until the search was repeated by Boudewijn Roukema in 2004. Astonishingly, this time correlated circles were found in six diametrically opposed pairs forming an icosahedral pattern in the sky. The angular sizes of these circles were found to be 11±1°. A full description of the methods used and the results obtained is found in [7].

4.3   Cosmic Crystallography

A completely different way to determine the multiply connectedness of space is to analyse the distribution of distances between randomly chosen objects in the sky. In an infinite space this distribution should be essentially uniform, but

cut off by the horizon. In a finite space of significantly smaller radius than the observable universe, however, there are also non-zero distances from an object to itself. These distances occur at least once for each object in the sky close enough to show its next "copy" and would therefore produce a peak in the distance distribution[3]. The exact location of this peak will even contain information regarding the size of the universe. There is a slight catch to this method, in that these peaks will only occur if the symmetries of space producing ghost images are Clifford translations (translations followed by a rotation around the direction of translation). The relevant symmetries *are* Clifford translations in both Euclidean and spherical space, though, so this catch can largely be ignored here. If one is to investigate the possibility of multiply connected hyperbolic space, some adaptation to the method have to be made, complicating the procedure and rendering it unstable to measurement error[4].

This measurement technique has, like the circles in the sky method, been used in practice to determine the topology of space. The results of this actual search were rather lacking though, since reliably measured distances are scarce for objects more distant from earth than about 600 Mpc. This does provide a lower limit for the radius of space, but this lower bound had by 1996, when the search was done, already been reached by other methods. Concludingly, this method will only be able to contribute to the determination of the topology of comoving space if space is non-hyperbolic and if sufficient distance measurements become available in the future.

4.4 Suppression of the CMB quadrupole and the Eigenmodes of Space

Another very significant effect of multiply connected space lies in the boundary conditions it sets for global fields and waves. For this effect to be noticeable, a field needs to be found which behaves essentially as a closed system and the waves of which have had the time to cross space in its entirety. Preferably the waves of this field needs to be governed by some simple differential operator, ideally a Laplacian. Luckily such a field can be found in the CMB, the fluctuations or waves of which have been produced by acoustic perturbations of the primordial matter. These sound waves have had plenty of time to circumnavigate space, if it is multiply connected, and will therefore neatly be described in terms of standing waves of the space manifold. The boundary conditions completely govern the shape of these standing waves, and vice versa the shape of these standing waves can be used to determine the shape of space.

Waves in a multiply connected space can be described as lying on a fundamental domain of the space. From this fundamental domain description, it is clear that waves can only exist with wavelengths smaller than the diameter of such a domain. In the limit of a very large fundamental domain, multiply connected space should on small scales behave like its universal cover. This also means that the small wavelength waves of a multiply connected space should be very much like the small wavelength waves of the universal cover. This behaviour is clearly illustrated by the 1 dimensional case. The eigenfunctions of

the Laplacian on $\mathbb{R}$ are $e^{\pm ikx}$ for eigenvalue $-k^2$. On the circle $S^1 \cong \mathbb{R}/\mathbb{Z}$, we only have the solutions $e^{\pm ikx}$ for which $e^{\pm ik1} = e^{\pm ik0}$ or $k = 2\pi n$. So whereas clearly any wave on a multiply connected space is a wave on its universal cover, only "universal" waves with the symmetry of the space itself are waves in this space. In the 1 dimensional case these are the waves with wavelength $\frac{1}{2\pi n}$ for any $n \in \mathbb{N}$, which is a far smaller set than $\mathbb{R}_{>0}$ but does have 0 as a limit point. The point here is that the main difference in the spectra lies in the waves corresponding to wavelength of order 1. This means that a cut-off in waves down from a certain frequency is a clear sign of multiconnectedness of space. A fact, that to the author's knowledge has not been explained beyond direct computational confirmation, is that this surpression of low order moments in multiply connected spaces exists only in what are called well proportioned spaces[12]. For badly proportioned spaces, were the width of the space depends heavily on the direction, a surpression of high order moments occurs. This surpression can even outperform the surpression of lower order terms due to muliconnectness, in extreme cases. This means that a cut-off of low order moments in the CMB is a feat, not of general multiply connected spaces, but of a subclass thereoff, a member of which is the PDS.

Surprisingly, a cut-off of this sort does occur in the CMB. The explanation is generally sought in measurement errors like unaccounted for beam asymetries[1], as opposed to cosmological factors. The fact remains however, that no satisfying non-cosmological explanation exists at this moment, so explaining this anisotropy is a real merit for any model of the universe.

Different spaces are different quotients of their universal cover, so they also allow different subsets of functions on this universal cover. This means that there would be different patterns of waves allowed in different spaces. Jean–Pierre Luminet and others have calculated the temperature fluctuations expected for some different spaces, both simply and multiply connected, and have found the best fit to be the PDS.

The parameters of the PDS were fitted to the temperature fluctuations in the $l = 4$ term, the results are shown in figure 6. Two terms, disregarding the term used to provide the parameters, in the Fourier expansion of the CMB seem to be significantly better fitted by the PDS than by the Euclidean model. Two terms is a rather small amount, and one could certainly hope for another explanation for their deviance from the concordance model. Still, as long as this explanation is not provided, the PDS model does manage to explain data the Euclidean model cannot, which is, to be honest, its first real scientific merit. A further complicating factor is that the curvature used by Luminet to fit the PDS to the data lies almost 2 standard deviations from the currently accepted curvature of space[6]. If this deviation from the mean increases any further by more precise measurements of the curvature of space, this fit will quickly become useless.

Making up the odds, the physical evidence for multiply connected space rests on fitting the CMB quadrupole. Where the circles in the sky method has only produced some very controversial, and all other tests have failed to provide any results in favour of multi connected space, the CMB quadrupole remains
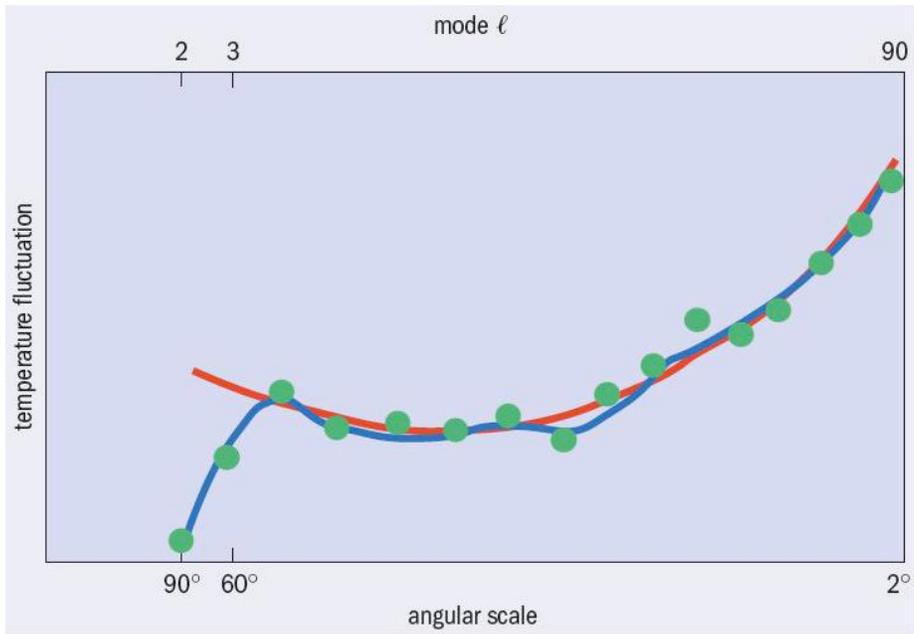
Figure 6: The fluctuations in temperature as a function of angle, or equivalently mode. The red line is the simply connected Euclidean fit, the blue line the PDS fit. This picture has been taken from [5]

anomalous in any simply connected case. While fitting the CMB anisotropies the best we can leads to the PDS as the most well-proportioned space, this is really the one and only argument there is.

5 Conclusion

The aim of this thesis has been to explore the possibility of multiconnectedness of space and to see whether physical traces can be found of such topologies. In section 2 a quick survey was given of the different topologies possible on geometric 3 manifolds. It turned out that 8 homogeneous geometries were possible of which only 3 are geometrically isotropic, being the well-known spherical, Euclidean, and hyperbolic spaces. Hyperbolic space allows the broadest range of quotient spaces to be formed, but is slightly disfavoured by curvature measurements. From a topological point of view there are quite a lot of hyperbolic 3 manifolds, which can therefore all be rejected as models for the universe. History seems to have chosen Euclidean space to be the space that we inhabit as is expressed in the concordance model of cosmology. Whereas the concordance model assumes a simply connected space, there are actually 10 topologically different 3 manifolds admitting Euclidean geometry. Since evidence seems to indicate a slightly spherical universe, though, this case was most extensively studied. Spherical manifold are much more abundant than Euclidean manifolds, but only the Poincaré Dodecahedral Space was given extensive treatment in section 3. In section 3, a proof was given for the correctness of the generally used construction or description of the PDS. The PDS is described as the quotient of the sphere by the action of the binary icosahedral group, which is shown to be equivalent to identifying faces of a dodecahedron with minimal relative twist. In section 4, a variety of ways was discussed for testing for multiconnectedness in general, but PDS topology in particular. Most of the actual measurements done are inconclusive at best, and the last decade has seen a perpetual reduction of the possibility of multi connected space, at least with a characteristic length smaller than the observable universe. In conclusion to this, the PDS is far from proven to be shape of the universe, but should be considered the best bet, as long as it explains the CMB quadrupole anomaly better than any other space.

Acknowledgements

While writing this thesis, I have enjoyed more support and understanding than I could have wished for from more people than I can mention. To these people I would hereby like to express my gratitude and my sincere hope, that in their eyes the end product has justified this support.

Two people I would like to name explicitly are both my thesis advisors, Mees de Roo and Gert Vegter, without whom this thesis would never have seen the light of day.

References

[1] C.L. Bennett et al. Seven-year Wilkinson microwave anisotropy probe (WMAP) observations: Are there cosmic microwave background anomalies? 2010.

[2] Neil J. Cornish, David N. Spergel, and Glenn D. Starkman. Circles in the sky: Finding topology with the microve background radiation. 1996.

[3] R. Lehoucq, M. Lachièze-Rey, and J.P. Luminet. Cosmic crystallography. 1996.

[4] Roland Lehoucq, Jean-Philippe Uzan, and Jean-Pierre Luminet. Limits of crystallographic methods for detecting space topology. 2000.

[5] Jean-Pierre Luminet. A cosmic hall of mirrors. 2005.

[6] Jean-Pierre Luminet. The shape of space after WMAP data. 2005.

[7] Boudewijn F. Roukema, Bartosz Lew, Magdalena Cechowska, Andrzej Marecki, and Stanislaw Bajtlik. A hint of Poincaré dodecahedral topology in the WMAP first year sky map. 2004.

[8] Svend E. Rugh and Henrik Zinkernagel. Weyl's principle, cosmic time and quantum fundamentalism. 2010.

[9] Peter Scott. The geometries of 3-manifolds. *Bulletin of the London Mathematical Society*, 15:401–487, 1983.

[10] William P. Thurston. *Three-Dimensional Geometry and Topology*, volume 1. Princeton University Press, 1997.

[11] C. Weber and H. Seifert. Die beiden Dodekaederräume. *Mathematische Zeitschrift*, 37:237–253, 1933.

[12] Jeffrey Weeks, Jean-Pierre Luminet, Alain Riazuelo, and Roland Lehoucq. Well-proportioned universes surpress CMB quadrupole. 2008.

[13] Joseph A. Wolf. *Spaces of Constant Curvature*. 3 edition, 1974.